Anal. Chem. **2001,** *73,* 2875−2882

An Acetylcholinesterase/Choline Oxidase-Based Amperometric Biosensor as a Liquid Chromatography Detector for Acetylcholine and Choline Determination in Brain Tissue Homogenates

Antonio Guerrieri† and Francesco Palmisano*

Dipartimento di Chimica, Università degli Studi di Bari, Via Orabona, 4-70126 Bari, Italy

A liquid chromatography (LC) detector based on a fast response and sensitive bienzyme amperometric biosensor for acetylcholine (ACh) and choline (Ch) is described. The detector fabrication consisted of glutaraldehyde co-cross-linking of acetylcholinesterase and choline oxidase with bovine serum albumin on the Pt working electrode of a conventional thin-layer electrochemical flow cell. The influence of some experimental parameters (e.g., enzyme loading, thickness of the bienzyme layer, flow rate) on the detector characteristics has been studied in order to optimize the analyte response while minimizing band-broadening and distortion. A mobile phase consisting of a phosphate buffer (*I*, 0.1 M; pH, 6.5) containing 5 mM sodium hexane sulfonate and 10 mM tetramethylammonium phosphate was found to give very satisfactory resolution and peak shape in ion-pair, reversed-phase LC. Linear responses were observed over at least four decades and absolute detection limits (at a signal-to-noise ratio of 3) were 12 and 27 fmol injected for Ch and ACh, respectively. After one month of intensive use in the LC system, the detector retained about 70% of its initial sensitivity. The potential of the described approach is demonstrated by the simultaneous determination of Ch and ACh in rat brain tissue homogenates.

Liquid chromatography (LC) is nowadays one of the analytical techniques most employed to analyze complex matrixes such as biological fluids. Although many compounds of biological significance can be chromatographically separated, a number of them are poorly (or not at all) detectable by common LC detectors as a result of the lack of, for example, chromophores or electroactive groups. A common approach to overcome this drawback relies on a pre- or postcolumn derivatization reaction leading to analyte derivatives with improved detectability.[1]

When analytes are inherently difficult to derivatize or a highly selective detection is required, a significant improvement can be achieved by postcolumn enzymatic reaction (PER) to "specifically" convert the analyte into an easily detectable product.[2] The LC-PER determination of acetylcholine (ACh, an important neurotransmitter of the cholinergic system) and choline (Ch, precursor and metabolite of ACh) is certainly a significant example of such an approach. ACh and Ch, separated by LC, were mixed in a reaction coil (see Scheme 1a) with a derivatizing solution containing acetylcholinesterase (AChE) and choline oxidase

Scheme 1. Detection Schemes Used in the Enzymatic Derivatization Methods[a]

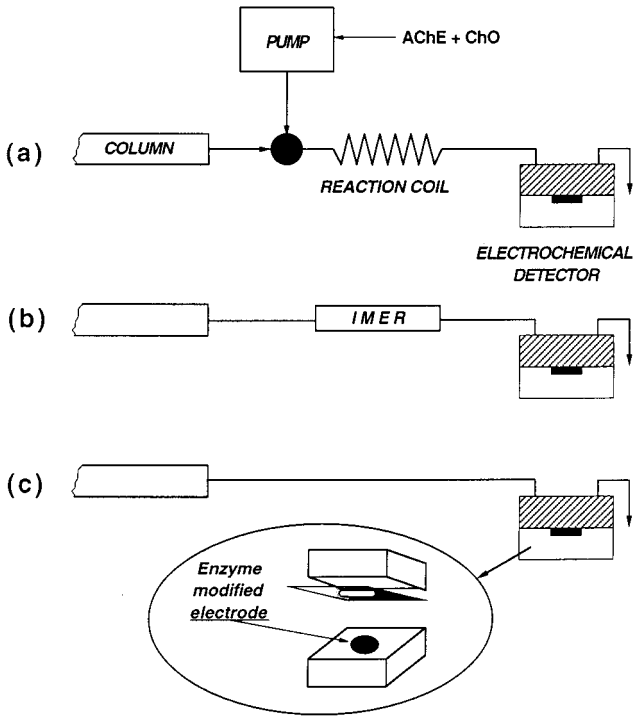

[a] (a) Homogeneous postcolumn enzymatic reaction (PER); (b) heterogeneous enzymatic reaction by immobilized enzyme reactor (IMER); (c) in situ reaction/detection by enzyme-modified electrode.

* Corresponding author: Fax: +39 080 5442026. E-mail: palmisano@chimica.uniba.it.

† Dipartimento di Chimica, Università della Basilicata, Via N. Sauro, 85-85100 Potenza, Italy.

(1) Poole, C. F.; Schuette, S. A. *Contemporary Practice of Chromatography*; Elsevier: 1984.

(2) Gorton, L.; Marko-Varga, G.; Dominguez, E.; Emneus, J. In *Analytical Applications of Immobilized Enzyme Reactors*; Lam, S., Malikin, G., Eds.; Blackie Academic & Professional: 1994; Chapter 1, p 1.

10.1021/ac000852h CCC: $20.00
Published on Web 06/06/2001

(ChO) and H_2O_2 enzymatically produced according to the following reactions

$$\mathrm{ACh} + \mathrm{H_2O} \xrightarrow{\mathrm{AChE}} \mathrm{Ch} + \text{acetic acid}$$

$$\mathrm{Ch} + 2\mathrm{O_2} + \mathrm{H_2O} \xrightarrow{\mathrm{ChO}} \text{betaine} + 2\mathrm{H_2O_2}$$

measured by electrochemical detection (ED) at a Pt electrode.[3] The result is a powerful combination of the separating power of LC, the specificity of enzymatic reactions, and the sensitivity and selectivity of the ED.

Homogeneous postcolumn derivatization, however, suffers from some drawbacks, such as an increased complexity in the LC setup, a large amount of enzymes wasted, a limited stability, and the high cost of soluble enzymes. In this respect, a significant improvement is represented by the use of immobilized enzyme reactors (IMERs), thus reaching the goals of simplifying the experimental setup (see Scheme 1b), improving enzyme stability, and reducing the analysis cost.[2] Adsorption on the ion-exchanger stationary phase,[4] cross-linking on alkylamino-bonded silica,[5−8] covalent binding on CNBr-activated sepharose[9,10] or through avidin−biotin complexation and antibodies specific to the enzymes,[11] as well as physical methods[12] have been used for AChE and ChO immobilization, mainly in packed-bed-type IMERs.

Apart from difficulties that are intrinsic to enzyme immobilization, a thorough optimization of the LC-IMER setup is often necessary:[2] IMER should be designed to attain a high conversion efficiency, thus minimizing band-broadening.[13] To achieve complete conversion and to improve the IMER stability, large enzyme amounts are usually immobilized; however, high enzyme loadings do not necessarily ensure a high activity, because multilayers of bound protein can slow the enzyme kinetics.[13] Moreover, an increase in the reactor length to increase the enzymatic conversion efficiency adversely affects band-broadening and may result in unacceptable chromatographic resolutions.[13] Attempts to minimize band-broadening by using beds of small-size particles can set a further limit to the reactor length because high back-pressures may also affect the catalytic properties of the immobilized enzyme.[2] A further drawback can also derive by the interaction of the analyte with the bed support (e.g., glass, silica), which leads to nonlinear chromatographic behaviors causing severe peak tailing or splitting effects in the case of ACh and Ch.[14]

An alternative approach to IMER-ED coupling for LC detection of Ch and ACh could be represented by an amperometric biosensor based on immobilized AChE and ChO enzymes; however, examples of such an approach are difficult to find, although several applications of amperometric biosensors as LC detectors have been described.[15−19] This likely could be ascribed to the fact that most ACh/Ch amperometric biosensors described so far[20] are not sufficiently sensitive, cannot be easily adapted or incorporated into low-volume flow cells of well-defined (e.g., thin-layer or wall-jet) geometry or do not satisfy one of the fundamental requirements of a LC detector, that is, a very low response time.

We have recently developed[21,22] a sensitive and fast-response amperometric biosensor for ACh and Ch on the basis of AChE and ChO being immobilized on a Pt electrode by glutaraldehyde co-cross-linking with bovine serum albumin (BSA). The immobilization procedure proved simple, fast, and easily adaptable to typical working electrodes employed in conventional flow cell of LC electrochemical detectors.

This paper describes the performances of such a biosensor as an amperometric detector for flow injection (FI) and LC systems and demonstrates the feasibility of an alternative approach to the above-described LC-IMER-ED method in which the IMER-ED is replaced by an immobilized enzyme amperometric biosensor, that is, by a detector coupling in the same physical device the postcolumn enzymatic reaction and the electrochemical detection of the enzymatically produced H_2O_2 (see Scheme 1c). The simultaneous determination of Ch and ACh in rat brain tissue homogenates by ion-pair, reversed-phase LC is also described, and the merits of the present approach are discussed.

EXPERIMENTAL SECTION

Reagents. Choline chloride, acetylcholine chloride, choline oxidase (EC 1.1.3.17 from *Alcaligenes spp.*, 14.6 U/mg solid), cholinesterase acetyl (EC 3.1.1.7, type VI-S, from electric eel, 225 U/mg solid), bovine albumin (fraction V), glutaraldehyde (grade II, 25% aqueous solution), 1-pentanesulfonic acid, 1-hexanesulfonic acid, 1-heptanesulfonic acid, and 1-octanesulfonic acid sodium salts were all purchased by Sigma (Sigma Chemical Co.; St. Louis, MO) and used without further purification. Tetramethylammonium and tetraethylammonium phosphate solutions were prepared by neutralizing tetramethylammonium and tetraethylammonium hydroxides (both Sigma), respectively, with H_3PO_4 (Analyticals, Carlo Erba; Milan, Italy). Choline chloride was dried under vacuum over P_2O_5. All of the other chemicals were of analytical reagent grade. Solvents were HPLC grade. Carrier stream and mobile phase were filtered through a 0.45-μm filter (HATF Millipore; France). Ch and ACh stock solutions were prepared in tridistilled water, carrier stream, or mobile phase and stored

(3) Potter, P. E.; Meck, J. L.; Neff, N. H. *J. Neurochem.* **1983**, *41*, 188−194.
(4) Eva, C.; Hadjiconstantinou, M.; Neff, N. H.; Meek, J. L. *Anal. Biochem.* **1984**, *143*, 320−324.
(5) Yao, T.; Sato, M. *Anal. Chim. Acta* **1985**, *172*, 371−375.
(6) Kaneda, N.; Asano, M.; Nagatsu, T. *J. Chromatogr.* **1986**, *360*, 211−218.
(7) Tyrefors, N.; Gillberg, P. G. *J. Chromatogr.* **1987**, *423*, 85−91.
(8) Damsma, G.; Van Bueren, D. L.; Westerink, B. H. C.; Horn, A. S. *Chromatographia* **1987**, *24*, 827−831.
(9) Van Zoonen, P.; Gooijer, C.; Velthorst, N. H.; Frei, R. W. *J. Pharm. Biomed. Anal.* **1987**, *5*, 485−492.
(10) Teelken, A. W.; Schuring, H. F.; Trieling, W. B.; Damsma, G. *J. Chromatogr.* **1990**, *529*, 408−416.
(11) Gunaratna, P. C.; Wilson, G. S. *Anal. Chem.* **1990**, *62*, 402−407.
(12) Flentge, F.; Venema, K.; Koch, T.; Korf, J. *Anal. Biochem.* **1992**, *204*, 305−310.
(13) Marko-Varga, G.; Gorton, L. *Anal. Chim. Acta* **1990**, *234*, 13−29.
(14) Tyrefors, N.; Carlsson, A. *J. Chromatogr.* **1990**, *502*, 337−349.
(15) Emneus, J.; Marko-Varga, G. *J. Chromatogr., A* **1995**, *703*, 191−243.
(16) Belay, A.; Ruzgas, T.; Csoregi, E.; Moges, G.; Tessema, M.; Solomon, T.; Gorton, L. *Anal. Chem.* **1997**, *69*, 3471−3475.
(17) Horiuchi, T.; Torimitsu, K.; Yamamoto, K.; Niwa, O. *Electroanalysis* **1997**, *9*, 912−916.
(18) Liden, H.; Buttler, T.; Jeppsson, H.; Marko-Varga, G.; Volc, J.; Gorton, L. *Chromatographia* **1998**, *47*, 501−508.
(19) Larsson, N.; Ruzgas, T.; Gorton, L.; Kokaia, M.; Kissinger, P.; Csoregi, E. *Electrochim. Acta* **1998**, *43*, 3541−3554.
(20) Kano, K.; Morikage, K.; Uno, B.; Esaka, Y.; Goto, M. *Anal. Chim. Acta* **1994**, *299*, 69−74.
(21) Zambonin, P. G.; Guerrieri, A.; Palmisano, F. *Euroanalysis VIII, Book of Abstracts*; Edinburgh, U.K., September 5−11, 1993.
(22) Guerrieri, A.; De Benedetto, G. E.; Palmisano, F.; Zambonin, P. G. *Analyst* **1995**, *120*, 2731−2736.

in the dark at 4 °C. Dilute solutions were prepared just before their use.

Apparatus. FI and LC experiments were performed by using a Perkin−Elmer (Norwalk, CT) series 10 pump module, a Rheodyne (Cotati, CA) model 7125 injection valve equipped with a 20-μL loop, and an EG&G model 400 electrochemical detector. The latter included a thin-layer electrochemical cell with two 0.005-in.-thick gaskets (Bioanalytical Systems, Inc.; West Lafayette, IN), a Pt working electrode, and a Ag/AgCl, 3M NaCl reference electrode. Signals were recorded by a Kipp & Zonen (Delft, Holland) model BD 112 flatbed recorder.

In FI experiments, a chromatographic column (5-μm packing, 250 × 4.6 mm) was fitted between the pump and the injection valve to ensure proper operation of the pump pulse damper. A long and narrow PTFE tubing (0.5 mm i.d.) was used to connect the sample injection valve to the electrochemical cell and to ensure a Gaussian concentration profile.

Preparation of Modified Electrodes. Before each electrode modification, the Pt working electrode was cleaned by hot HNO_3 followed by an alumina (0.05-μm particles) polishing procedure, extensive washing, and sonication in tridistilled water.

AChE/ChO bienzyme electrodes were prepared as follows. A 300-μL aliquot of a phosphate buffer (*I*, 0.1 M; pH, 6.5) containing 16 mg BSA, 1 mg AChE, and 1 mg ChO amounts were carefully mixed with 30 μL of a glutaraldehyde 2.5% solution (obtained by dilution with phosphate buffer). Typically, 3 μL of the resulting solution was carefully spread out onto the electrode surface and air-dried at room temperature; after a few minutes, the enzyme electrode was ready to use. After their preparation, biosensors were flushed with the FI carrier or LC mobile phase to remove weakly bound or adsorbed enzyme and to swell the enzyme layer; usually, no more than 30 min was necessary to obtain a stable and steady-state response. When not in use, biosensors were stored in a phosphate buffer (*I*, 0.1 M; pH, 6.5) at 4 °C in the dark or left in the FI or LC system at 0.1 mL/min. Thickness measurements (on five biosensors) of the bienzyme-layer were performed as described elsewhere;[22] layers obtained with casting volumes of 3, 5, and 10 μL resulted in measurements of (9.5 ± 2.1), (20.0 ± 1.4), and (41.0 ± 3.6) μm thick, respectively. Enzyme-free membranes displayed thickness values not significantly different from these measurements.

Preparation of Rat Brain Homogenates. Male Fischer 344 rats (12 months old) were anesthetized with ethyl ether and then decapitated by guillotine. Two whole brains (2.8 g) were quickly homogenized with 14 mL of a 0.2 M $HClO_4$ solution by a potter, centrifuged at 10 000*g* for 15 min, and the resulting supernatant was stored at −20 °C in the dark. Before analysis, a sample aliquot was thawed, and the pH was adjusted to around neutrality by adding solid K_2HPO_4. After centrifugation and filtering through a 0.45-μm Millipore membrane, a 2-μL volume was typically injected.

FI and LC Conditions. The H_2O_2 detection potential was +0.65 V vs Ag/AgCl and, unless otherwise stated, the electrochemical detector time constant was set at 0.1 s. The FI carrier stream was a phosphate buffer (*I*, 0.1 M; pH, 6.5). LC was performed on a 5-μm Supelcosil (Supelco, Bellefonte, PA) LC-18-DB ODS column (250 × 2.1 mm) protected by a 20 × 2.1-mm precolumn with the same packing. The mobile phase was 5 mM 1-hexanesulfonic acid sodium salt and 10 mM tetramethylammonium phosphate in a potassium phosphate buffer (*I*, 0.1 M; pH, 6.5). Temperature was ambient. Flow rates and injection volumes are specified in the figure legends.

RESULTS AND DISCUSSION

Dynamic Behavior of the Detector. Conventional amperometric biosensors typically require[23] up to three discrete, macroscopic membranes, each performing a dedicated function (e.g., enzyme immobilization, electrode protection, and diffusional barrier). Integration of such devices with FI and LC systems usually also involves the fabrication of unconventional electrochemical flow cells having tailored geometry and often requires dedicated physical and chemical manipulations for its fabrication.[16,19,20,24,25] The multilayered structure and the complex diffusion pattern are responsible for significantly high response times (*RT*) that cause unacceptable distortions of FI and LC peaks. Indeed, severe peak tailing phenomena taking several minutes for the response to return to the baseline are reported.[26,27] Obviously, peak distortion and band-broadening have a significant impact on the sample throughput and carry-over in FI analysis and on resolution in LC, and in both cases, they adversely affect sensitivity.

In the present approach, immobilization of AChE and ChO on the working electrode of a commercially available electrochemical flow cell was simply achieved[21,22] by glutaraldehyde co-cross-linking with BSA. A bienzyme layer, strongly adhered onto the Pt surface to be very stable in flowing solutions, was obtained with no need for surface modification, such as Pt silanization.[26,28] The low thickness (∼10−40 μm, depending on the casting volume) of the membrane and its favorable diffusivity characteristics ensured fast *RT* in the low second range, as measured by batch experiments following a step change in the analyte concentration.[21,22]

The dynamic behavior of the biosensor in flowing systems (such as FI and LC), where a steady-state could not necessarily be achieved because of the sign inversion of the concentration gradient (at the membrane−solution interface) occurring at peak time, has been investigated. To distinguish between diffusional and enzyme kinetic limitations, two different sets of FI experiments were performed to detect H_2O_2 (i.e., the product of the enzymatic reaction) and Ch (or ACh) at enzyme-free and AChE/ChO membrane electrodes, respectively. Figure 1 compares the current−time profiles due to H_2O_2 injections at bare and enzyme-free membrane electrodes of different thickness. According to previous findings,[29] passing from bare to membrane-covered Pt electrodes, a decrease in peak current, a significant band-broadening, and a lag time were observed (see Figure 1), whose magnitude increased on increasing the membrane thickness. Interestingly, the ratio between peak currents at membranes and

(23) Cass, A. E. G., Ed. *Biosensors: A Practical Approach*; Oxford University Press: 1990.
(24) Buttler, T. A.; Johansson, K. A. J.; Gorton, L. G. O.; Marko-Varga, G. A. *Anal. Chem.* **1993**, *65*, 2628−2636.
(25) Marko-Varga, G.; Johansson, K.; Gorton, L. *J. Chromatogr., A* **1994**, *660*, 153−167.
(26) Nordling, M.; Elmgren, M.; Stahlberg, J.; Petterson, G.; Lindquist, S. E. *Anal. Biochem.* **1993**, *214*, 389−396.
(27) Ortega, F.; Dominguez, E.; Burestedt, E.; Emneus, J.; Gorton, L.; Marko-Varga, G. *J. Chromatogr., A* **1994**, *675*, 65−78.
(28) Yao, T.; Wasa, T. *Anal. Chim. Acta* **1988**, *209*, 259−264.
(29) Breen, W.; Cassidy, J. F.; Lyons, M. E. G. *Anal. Chem.* **1991**, *63*, 2263−2268.

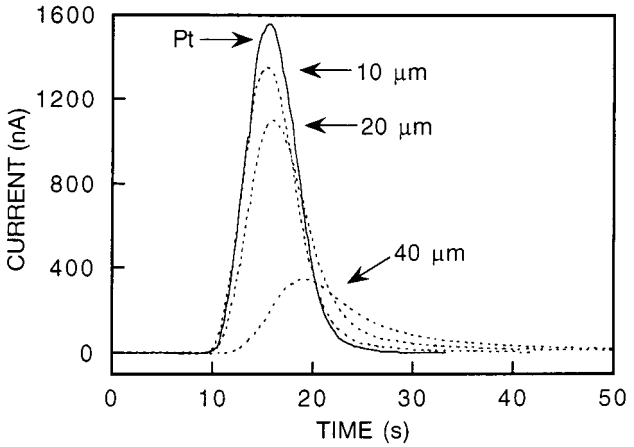

Figure 1. Dotted lines: flow injection responses for H_2O_2 (20 nmol injected) at a Pt disk electrode (thin-layer configuration) modified with enzyme-free membranes of several thickness. Continuous line: flow injection response at a bare Pt electrode. Flow rate, 1 mL/min; injected volume, 20 μL. Other conditions as described in the Experimental Section.

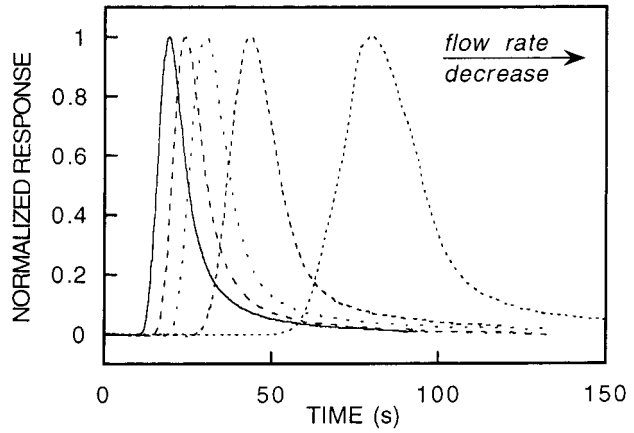

Figure 2. Flow injection responses relevant to H_2O_2 injection at several flow rates at a Pt disk electrode modified with a ~40-μm-thick enzyme-free membrane. Flow rates (left to right peaks): 1, 0.8, 0.6, 0.4, and 0.2 mL/min. Other experimental conditions as in Figure 1.

bare electrodes decreased with an increasing flow rate except for the thinnest (i.e., ~10 μm thick) membrane electrode, for which it remained almost constant. The lag time increased on when the membrane thickness (see Figure 1) or the flow rate for the thicker membrane electrodes increased, but it remained negligibly small, whatever the flow rate, at the thinnest membrane electrode. Finally, as Figure 2 shows, peak distortion/broadening decreased when the flow rate was decreased, even for thicker membranes. All of these features suggest a steady-state attainment in the experiment time domain only at the membrane−solution interface of the thinnest membrane; moreover, the flow rate dependence denotes that both the transport into the solution and the membrane permeability are rate-limiting under these conditions. These findings indicated also that membranes thicker than 10 μm introduced an appreciable diffusional barrier that is responsible for distortion/broadening of FI peaks. On the contrary, though, the thinnest membrane essentially gave rise only to a current lowering (a few percent, as compared with bare Pt) and is quite satisfactory for applications in flowing systems.

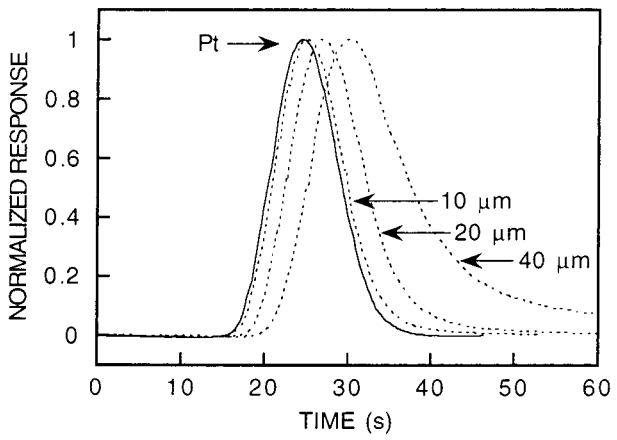

Figure 3. Dotted lines: normalized flow injection responses to Ch (1 nmol injected) at a Pt disk electrode (thin-layer configuration) modified with AChE/ChO membranes of several thicknesses. Continuous line: flow injection response to H_2O_2 at a bare Pt electrode. Flow rate, 0.6 mL/min. Other conditions as described in Figure 1 and in the Experimental Section.

A similar behavior was also observed (see Figure 3) in the case of bienzyme membrane electrodes in which enzyme substrates must partition and diffuse into the membrane generating H_2O_2, which is in part electrooxidized and in part lost into the flowing solution. Peak distortion/broadening and lag time for Ch (ACh behaving similarly) were found strongly dependent on the membrane thickness, confirming the diffusional constraints described above; however, in agreement with previous findings,[22] the peak current increased with membrane thickness and decreased when increasing the flow rate (vide infra). This behavior is expected[30−32] when the rate of enzyme catalysis is comparable to or slower than substrate diffusion. Then a compromise must be achieved between sensitivity and peak distortion/broadening; the 10-μm-thick bienzyme membrane seemed the best-suited for this purpose.

To evaluate the time constant of the bienzyme electrode, a frequency domain study of FI responses was performed by using the well-known Fourier transform technique. Figure 4 compares the frequency responses relevant to bienzyme membrane electrodes of different thicknesses and bare Pt. As can be seen, the membrane modification involved a significant low-pass filtering of peaks, at least for the thickest membranes; in particular, increasing the membrane thickness decreased the bandwidth, but the response rolled off with an increased slope. These plots permitted the evaluation of the equivalent bandwidth Δf, that is, of the rectangular bandwidth of area equal to that of the overall frequency response; the time constant τ of the membrane/electrode system could be evaluated (see Table 1) by the following equation

$$\tau = 1/(2\pi\Delta f) \qquad (1)$$

As can be seen from Table 1, the thinnest bienzyme membrane electrode had a time constant only slightly higher than the bare

(30) Mell, L. D.; Malloy, J. T. *Anal. Chem.* **1975**, *47*, 299−307.
(31) Bartlett, P. N.; Whitaker, R. G. *J. Electroanal. Chem.* **1987**, *224*, 27−35.
(32) Bartlett, P. N.; Whitaker, R. G. *J. Electroanal. Chem.* **1987**, *224*, 37−48.

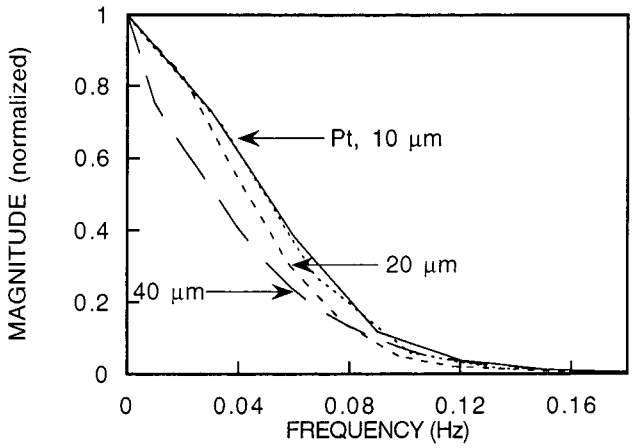

Figure 4. Frequency domain representation of flow injection responses shown in Figure 3. Continuous and dotted lines refer to H_2O_2 and Ch injections at bare and bienzyme membrane Pt electrodes, respectively. Other condition as described in Figure 3.

Table 1. Detector Time Constants τ[a] for Bare and Bienzyme Membrane Pt Electrodes[b]

	bienzyme membrane Pt electrode, μm		
bare Pt	10	20	40
2.9 ± 0.2	3.0 ± 0.1	3.6 ± 0.1	4.5 ± 0.1

[a] In seconds. [b] Data (from three different biosensors) refers to H_2O_2 (bare Pt) and Ch injections, as in Figures 3 and 4.

Pt electrode, demonstrating that the described electrode modification does not compromise the dynamic response of the detector, except for a slight decrease in peak height, as a consequence of restricted diffusion within the membrane.

Enzymatic Conversion Efficiency and Flow Rate Dependence. The enzymatic conversion efficiency (ECE) of an IMER is simply evaluated[4] by comparing the flow responses that are obtained when injecting known amounts of enzyme substrate and H_2O_2 (i.e., the enzymatic product) standards. ECE is mainly controlled by the residence time of the substrate inside the enzyme reactor and by the amount of the immobilized enzyme.[2] Because this latter can be very large, IMERs are usually capable of achieving a 100% ECE.[5,8] Obviously, this is not the case for an amperometric biosensor, for which the enzyme loading is usually much more lower. However, a 100% ECE does not necessary imply a 100% overall conversion efficiency, that is, one mole of electrons (obtained from H_2O_2 oxidation) per mole of enzyme substrate, because the detector is not coulometric. Indeed, the faradaic conversion efficiency (FCE) of a thin-layer amperometric detector is typically below 5% at flow rates usually used in LC analysis.[33]

In the present case, the ratio between Ch (or ACh) and H_2O_2 sensitivities at a typical bienzyme membrane electrode gave an ECE of ~3% at 0.2 mL/min, that is, about 30-fold lower than an IMER. However, the overall conversion efficiency for an amperometric biosensor depends on the enzymatic conversion as well as on the fraction of H_2O_2 produced inside the enzyme membrane,

(33) Duda, C. T.; Kissinger, P. T. In *Methods in Neurotransmitter and Neuropeptide Research, Part 1, 11 − Techniques in the Behavioral and Neural Sciences*; Parvez, S. H., Naoi, M., Nagatsu, T., Parves, S., Eds.; Elsevier Science Publishers: Amsterdam, 1993; pp 1−82.

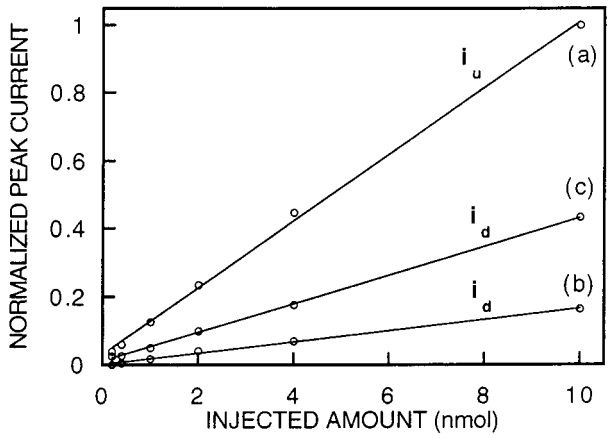

Figure 5. Normalized flow injection responses vs injected amount of Ch observed at an in-series, dual-electrode thin-layer cell whose upstream (u) and downstream (d) electrodes were a modified bienzyme and a bare Pt electrode, respectively. Curve a, upstream electrode responses. Curves b and c, downstream electrode responses recorded with the upstream electrode potentiostated at +0.65 V or disconnected from the potentiostat, respectively. Flow rate, 0.2 mL/min; injected volume, 20 μL. Other conditions as described in the Experimental Section.

which is electrooxidized at the electrode surface, the remaining part being lost in the flowing stream. To demonstrate H_2O_2 loss, a dual in-series Pt electrode thin-layer cell was used in which only the upstream electrode was modified by the bienzyme layer. Figure 5, curves a and b, showing peak currents observed at the upstream and downstream electrodes, respectively, upon injections of Ch standards, gives clear evidence of H_2O_2 loss from the bienzyme layer. Curve c shows peak currents that were observed at the downstream electrode when the upstream electrode, disconnected from the potentiostat, acted as an enzyme microreactor. Thus, the ratio between the slopes of curves c and b gave a rough estimate of the fraction of the biocatalytically generated H_2O_2 electrooxidized at the bienzyme electrode. In fact, assuming in a first approximation that the upstream, bienzyme electrode behaves in the same manner when electrically connected (on) or disconnected (off), the slopes of curves b and c can be written, respectively, as:

$$i_d^{on}/[\mathrm{Ch}] = k \cdot \mathrm{ECE} \cdot \mathrm{FCE_d} \cdot (1 - \mathrm{FCE_u}) \qquad (2)$$

$$i_d^{off}/[\mathrm{Ch}] = k \cdot \mathrm{ECE} \cdot \mathrm{FCE_d} \qquad (3)$$

where the u and d subscripts refer to the upstream and downstream electrodes, respectively, and k is a proportionality constant. Thus, FCE_u could be easily estimated to be ~0.6; because a 3% ECE was obtained, the overall conversion efficiency was near 2% which is only 2−3× lower than that expected for an IMER coupled to amperometric detection of H_2O_2.

The flow rate dependence for both Ch and ACh responses is shown in Figure 6. As can be seen, a decrease in the flow rate gave rise to a significant response increase for both analytes; the ECE (data not shown) also increased (e.g., up to 7% at 0.05 mL/min), while dual electrode experiments pointed out an increased H_2O_2 relative loss as the flow rate decreases. Flow rate dependence for enzyme membrane electrodes has been explained by citing

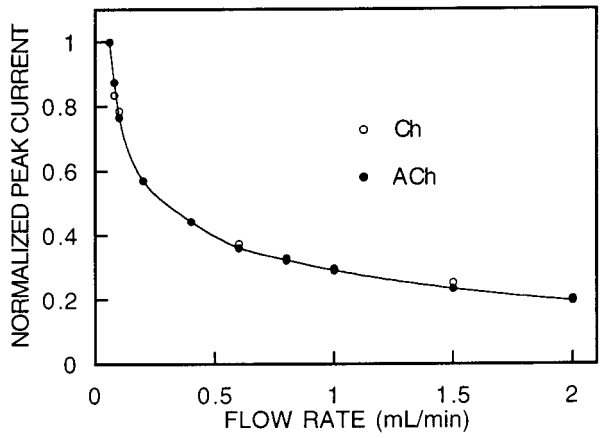

Figure 6. Normalized flow injection responses as a function of flow rate for Ch and ACh injections at the 1 nmol level. Injected volume, 20 μL. Other conditions as described in the Experimental Section.

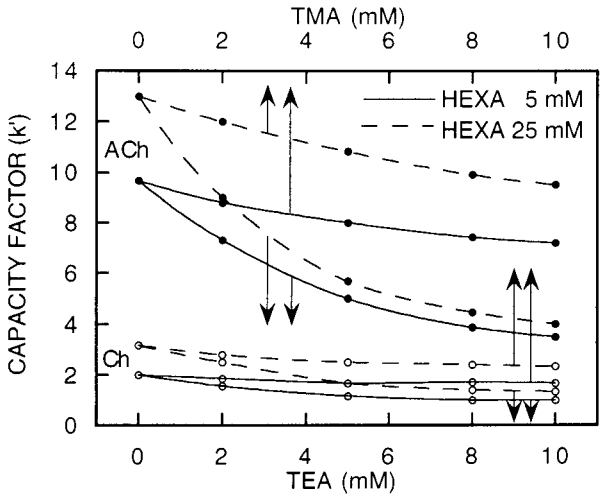

Figure 7. Capacity factors of Ch and ACh as a function of TEA or TMA concentrations at 5 mM (continuous lines) and 25 mM (dotted lines) HEXA in the mobile phase. Ch and ACh injected amounts, 500 pmol each; flow rate, 0.2 mL/min; injected volume, 2 μL. Other conditions as described in the Experimental Section.

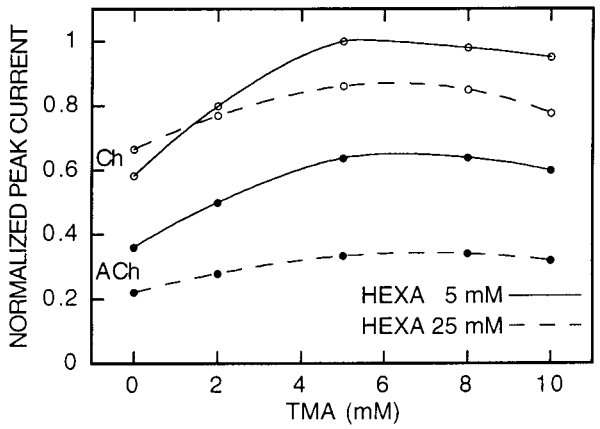

Figure 8. Normalized peak currents of Ch and ACh as a function of TMA concentration at 5 mM (continuous lines) and 25 mM (dotted lines) HEXA in mobile phase. Other conditions as in Figure 7.

either H_2O_2 build-up[32] in the diffusion layer or an increased residence time for the enzyme substrate in the flow cell;[34] the observed behavior seems consistent with the last assumption that the bienzyme electrode behaves like an enzyme reactor.

Chromatographic Separation and Analysis. Even if ion-pair RP-LC is the most used technique for Ch and ACh separation, conflicting results exist concerning the best chromatographic conditions. Indeed, this apparent contradiction is proof of the actual difficulties experienced in the separation of such quaternary ammonium compounds. In fact, as Salamon et al.[35] pointed out, the partition mechanism expected between the ion-paired analyte and the reversed stationary phase is complicated by ion-exchange interaction between the free analyte and the surface silanol groups, which in most cases gives rise to strong adsorption of both of the analytes,[5,11] producing irregular retention and band-broadening or peak-splitting. Although such effects can be minimized by end-capping of the stationary phase, by silanol blocking agents, and by adjusting the pH and ionic strength of the mobile phase,[4,5,7,10,11] the effectiveness of these approaches strongly depends on the surface density of silanol groups. This can vary greatly, depending on the column manufacter and the batch of silica, even from one lot number to another by the same manufacter. Finally, further complications can arise from the use of certain silanol blocking agents, for example, tetramethylammonium salts, which seem to inhibit both the soluble[3] and immobilized[5,11] forms of ChO.

As a matter of fact, a chromatographic study was necessary. A 2.1-mm-i.d. deactivated ODS column was used both to improve the peak shape and to decrease the operating flow rate, the column volume, and the sample dilution, thus increasing the detector sensitivity. The best conditions for the chromatographic separation and analysis of Ch and ACh were investigated by varying the concentration and the nature of several ion-pairing and silanol blocking agents in a mobile phase containing potassium ions, which are known to improve peak shape.[10] Among the ion-pairing agents here investigated, 1-hexanesulfonate (HEXA) gave the best results in terms of peak resolution, shape, and retention times. Tetramethylammonium (TMA) and tetraethylammonium (TEA) salts were found to affect the capacity factors of Ch and ACh (see Figure 7) as well as resolution and peak shape. Indeed, excellent peak shapes were observed using 5−10 mM TEA at 5 mM HEXA level; unfortunately, such an improvement was coupled to a significant signal depression (usually higher than 50%), probably as a result of some kind of enzyme inhibition. In agreement with other findings,[9] no inhibition effect was observed for TMA, because as Figure 8 shows, heights of both Ch and ACh chromatographic peaks increased on increasing the concentration of TMA in the mobile phase; TMA was then preferred to TEA.

Figure 9a shows a typical chromatogram relevant to a 100-fmol injection of Ch and ACh obtained with the mobile phase optimized as above-described. As can bee seen, both analytes were well separated in a few minutes with good resolution and sensitivity. The absolute detection limits for Ch and ACh (calculated at a signal-to-noise ratio of 3) were 12 and 27 fmol, respectively, for a 10-μL injection (corresponding to minimum detectable concentrations of 1.2 and 2.7 nM). These compare quite well even with the most sensitive LC-IMER-ED methods (see Table 2) based on wired peroxidase[36−38] electrodes to improve

(34) Centonze, D.; Guerrieri, A.; Malitesta, C.; Palmisano, F.; Zambonin, P. G. *Ann. Chim. (Rome)* **1992**, *82*, 219−234.
(35) Salomon, J.; Nguyen, P. T.; Remien, J. *J. Chromatogr.* **1992**, *596*, 43−49.

Table 2. Comparison of Some Analytical Techniques Used for Ch and ACh Analysis

methods	enzyme immobilization techniques	detection limit (S/N = 3) fmol Ch	fmol ACh	nM Ch	nM ACh	real sample applications	ref
LC-PER-ED	none	1000[a]	2000[a]			neuronal tissues	3
LC-IMER-ED	adsorption	5000[a]	5000[a]			brain extracts	4
	cross-linking	140	180	28	36	spinal cord microdialysates	7
	cross-linking		75[b]		3.8[b]	brain microdialysates	8
	CNBr-activated sepharose	50[a]	50[a]	2.5[a]	2.5[a]	cerebrospinal fluids	10
	avidin−biotin coupling	100[a,c]	100[a,c]	5[a]	5[a]	brain tissue homogenates	11
	physical entrapment	15[b]	22[b]	30[b]	45[b]	brain tissue homogenates and microdialysates, cerebrospinal fluids	12
	ChO pre-IMER + AChE/ChO IMER		5		5	brain microdialysates	39
	commercial IMER + wired peroxidase electrode	10	10	2	2	brain microdialysates	37
	solid-phase reactor + coulometric cell	20	20	2	2	brain microdialysates	40
	commercial IMER + ultramicroarray electrode	6	5.7	1.2	1.1	none	41
LC-IMER-CD[d]	CNBr-activated sepharose	500	700	25	28		9
GC-CI		1000[a]	1000[a]			brain extracts	42
LC-MS		5000[a]	2000[a]			brain tissue homogenates	43
LC-BIO[e]	cross-linking on microelectrodes	50[a]	50[a]	833[a]	833[a]	none	20
	co-cross-linking on thin-layer Pt cell	12	27	1.2	2.7	brain tissue homogenates	this study

[a] Signal-to-noise ratio not given. [b] Detection limits calculated at a signal-to-noise ratio of 3:1. [c] Detection limits of 10 fmol in FI analysis. [d] CD, chemiluminescence detection. [e] BIO, amperometric biosensor.

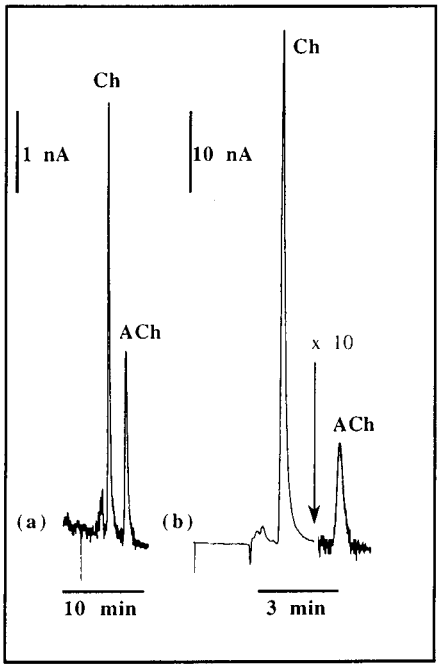

Figure 9. Chromatograms at the bienzyme amperometric detector relevant to (a) a standard of Ch and ACh (100 fmol each in mobile phase) and (b) a decapitated rat brain tissue homogenate (calculated Ch and ACh levels, 600 pmol/g and 2.9 pmol/g, respectively). Flow rate, 0.2 mL/min; injected volume, (a) 10 and (b) 2 μL; detector time constant, 2s. Other conditions as described in the Experimental Section.

H_2O_2 detection. Anyway, this latter suffers from intrinsic buffer and ionic strength dependence[36] and the needs of a stringent control of oxygen concentration in the mobile phase to reduce background currents.[37] Note, incidentally, that all of the approaches based on physically or chemically modified electrodes (see Table 2) appear to be the most effective at corroborating the idea that the IMER performance is not the crucial step in lowering Ch and ACh detection limits.

Calibration curves for both analytes were linear (correlation coefficients better than 0.9995) up to 5 nmol injected. The within-a-day ($n = 5$) coefficients of variation for Ch and ACh at a 100 pmol level were 2.8% and 4.0%, respectively, but between-days ($n = 6$) coefficients of variation resulted in 9.8% and 8.9%.

As far as the operational stability of the biosensor is concerned, after a month of intensive use in the LC system (and storage at 4 °C when not in use) about 70% of initial the sensitivity was still retained for both analytes.

Finally, Figure 9b shows a typical chromatogram of a brain tissue homogenate from decapitated rats. It is worth noting the absence of the large solvent front that usually needs to be removed by further prepurification steps[3,44] or by using a glassy carbon precolumn.[45] As expected[11,44,46] in the case of decapitated rat brain tissue analysis, very high Ch levels were observed (see Figure 9b); indeed such a post-mortem increase in Ch concentration

(36) Yang, L.; Janle, E.; Huang, T.; Gitzen, J.; Kissinger, P. T.; Vreeke, M.; Heller, A. *Anal. Chem.* **1995**, *67*, 1326−1331.
(37) Huang, T.; Yang, L.; Gitzen, J.; Kissinger, P. T.; Vreeke, M.; Heller, A. *J. Chromatogr.* B **1995**, *670*, 323−327.
(38) Kato, T.; Liu, J. K.; Yamamoto, K.; Osborne, P. G.; Niwa, O. *J. Chromatogr., B* **1996**, *682*, 162−166.
(39) Tsai, T. R.; Cham, T. M.; Chen, K. C.; Chen, C. F.; Tsai, T. H. *J. Chromatogr., B* **1996**, *678*, 151−155.
(40) Greaney, M. D.; Marshall, D. L.; Bailey, B. A.; Acworth, I. N. *J. Chromatogr.* **1993**, *622*, 125−135.
(41) Niwa, O.; Horiuchi, T.; Morita, M.; Huang, T.; Kissinger, P. T. *Anal. Chim. Acta* **1996**, *318*, 167−173.
(42) Khandelwal, J. K.; Szilagyi, P. I.; Barker, L. A.; Green, J. P. *Eur. J. Pharmacol.* **1981**, *76*, 145−156.
(43) Ishimaru, H.; Ikarasdhi, Y.; Maruyama, Y. *Biol. Mass Spectrom.* **1993**, *22*, 681−686.
(44) Ikarashi, Y.; Sasahara, T.; Maruyama, Y. *J. Chromatogr.* **1985**, *322*, 191−199.
(45) Ikarashi, Y.; Iwatsuki, H.; Blank, C. L.; Maruyama, Y. *J. Chromatogr.* **1992**, *575*, 29−37.
(46) Asano, M.; Miyaauchi, T.; Kato, T.; Fujimori, K.; Yamamoto, K. *J. Liq. Chromatogr.* **1986**, *9*, 199−215.

seems to be due[11] to the conversion of significant amounts of ACh to Ch by residual AChE in the tissue or to the release of membrane-bound Ch. Even with such high Ch levels, ACh quantification was still feasible, in contrast to previous reports[38,39] in which an immobilized ChO precolumn was required to eliminate the high endogenous Ch level interfering with ACh detection.

To confirm the identities of Ch and ACh chromatographic peaks, brain tissue homogenates were analized either at an enzyme-free membrane electrode or after preincubation with soluble AChE and ChO. In both cases, no peaks were observed at the retention times that were expected for the two analytes, thus confirming the high specificity of the method and the absence of chromatographic interference (note that some biogenic compounds are known[3] to chromatographically interfere with Ch and ACh analysis). In this respect, it is worth noting that a late-eluting peak (not shown in Figure 9b), possessing a retention time similar to that of dopamine was typically observed.

CONCLUSION

This is the first report showing that a LC detector based on a sensitive and fast-response AChE/ChO amperometric biosensor can effectively compete with conventional IMER-ED. The biosensor, fabricated by a simple co-cross-linking immobilization procedure on a conventional thin-layer electrochemical cell, shows a very low time constant and a satisfactory operational stability. Detection limits that were achieved compare well with those of the most sensitive LC-IMER-ED methods so far described.

The chromatographic step significantly hampers the overall analytical procedure and its ruggedness. The ultimate goal would be to devise a biosensor that is able to selectively and simultaneously detect Ch and ACh in complex matrixes with no need for a chromatographic step. Work in this direction is in progress in our laboratory.

ACKNOWLEDGMENT

Prof. P. G. Zambonin is gratefully acknowledged for helpful discussions. Work carried out with financial support from "CNR—Target Project on Biotechnology".

Received for review July 27, 2000. Accepted April 16, 2001.

AC000852H